1

Introduction

Powders or particulate matter are a commonly used type of raw material in many industrial processes due to their versatility and ease of handling (Mörl et al., 2007; Tsotsas and Mujumdar, 2011). Powders offer several advantages compared to other types of raw material, such as ease of transportation and storage, high surface area-to-volume ratio, and rapid reaction kinetics (Lowell, 2004). However, powders provide challenges such as poor flowability or dust formation (Baxter and Prescott, 2019). Different material powders can be mixed to create homogeneous formulations, which is crucial for achieving consistent product quality. Overall, the use of powders as raw materials in industrial processes has enabled the development of new and innovative products, while also improving process efficiency and reducing costs (Dobrzanski, 2017).

In many processes, the surface properties of the powdery raw materials are changed by the use of liquids. Typical processes utilizing liquids are spray granulation, spray agglomeration, encapsulation or coating. These processes are often carried out in so-called fluidized bed reactors, a special type of apparatus, which creates a dense gas-solid flow, in which the particulate matter behaves like a liquid, which improves the properties such as the flowability of the particles. These fluidized bed processes offer the possibility to finely tune the chemical and mechanical properties of the solid materials, resulting in the production of tailored particles that are suitable for a wide range of applications (Orth et al., 2023). Due to this versatility in the manufacturing of products, these processes are used in a variety of industries, such as the food industry (Dewettinck and Huyghebaert, 1999; Werner et al., 2007), the automotive industry (Kumar and Suman, 2021) and the pharmaceutical industry (Turton, 2008). An overview of different processes carried out in fluidized beds and the resulting products are shown in Figure 1.1. Particularly high demands are placed on the product quality in the manufacturing process of pharmaceutical products. One process that is used due to its advantages in producing high strength, spherical granules with optimal drug distribution (Korakianiti et al., 2004; Jacob, 2007), is the

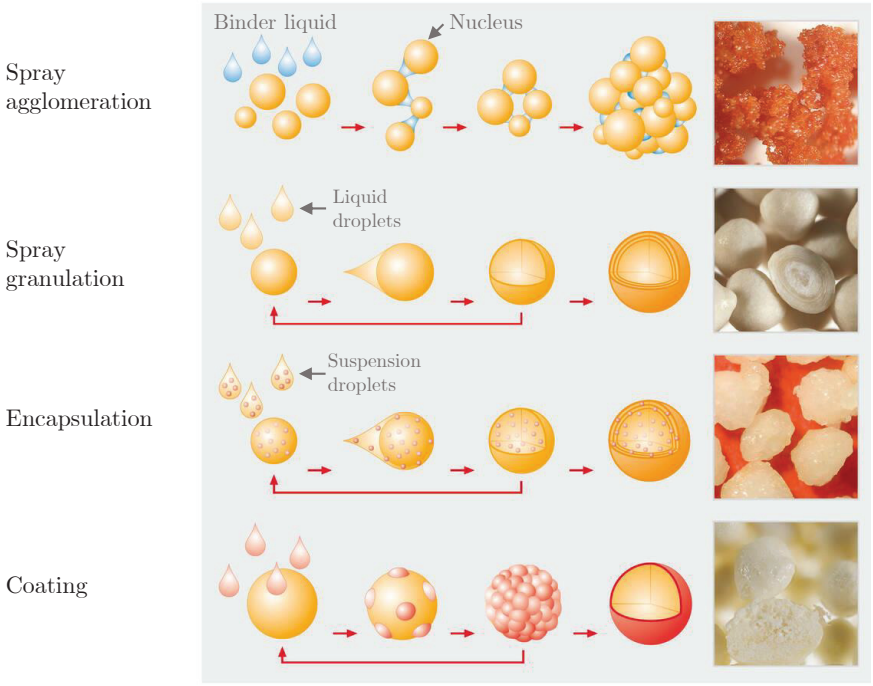

Figure 1.1: Examples of processes typically carried out in fluidized beds using binder fluid and a selection of images of the resulting products. (Glatt Ingenieurtechnik GmbH, 2022).

rotary granulation, which is investigated in detail in this work. In order to be able to estimate the quality and properties of the products based on the raw material and process parameters, it is of elementary advantage to precisely understand the processes at the particulate level. In the dense gas-solid flows discussed here, the process is mainly determined by inter-particulate collisions. Seville et al. (2000) as well as van Buijtenen et al. (2009) have shown that changes on micro-scale behavior lead to changes in the product properties and phenomena on the macro-scale.
In addition to the dynamics at the particulate level, the understanding of the liquid phase is fundamental in the above-mentioned processes, which led to a number of experimental investigations being carried out (L. Gu et al., 2004; Kristensen, 2005; Langner et al., 2020). However, the non-invasive investigation of gas-solid flows remains a challenge, as any kind of fixtures used to measure properties will cause a change in the flow, which in turn may affect the product properties.

1.1 Aim of this Work

In this work, experimental investigations are performed in a rotary granulator, which can be analyzed three-dimensionally, non-invasively using a new Magnetic Particle Tracking system. In particular, the investigations are intended to show the influence of parameters such as liquid on the dispersion behavior. Overall, the following scientific questions and tasks are to be carried out and answered in this work:

- Selection of suitable magnetic materials for the tracer particle for Magnetic Particle Tracking as well as production of bulk particles and subsequent comparison of the particle properties.
- Investigation of the measurement accuracy of the renewed Magnetic Particle Tracking measurement system as well as investigations of which variables significantly affect the measurement result.
- Comparison of experimental investigations in a rotary granulator with numerical simulations using CFD-DEM, especially with regard to the influence of added liquid in the particle bed.
- Investigation of stationary operating conditions with regard to the distribution of particle concentration and a range of velocities (tangential, radial, etc).
- Particular emphasis will be placed on the analysis of the experimental tests to characterize the dispersion behavior in the particle bed. For this purpose, different dispersion models will be applied and compared.
- Verification of the first-time applicability of the Magnetic Particle Tracking technology to measure transient process conditions during rotor granulator experiments.

1.2 Structure of this Work

In this thesis, experimental investigations are carried out in a rotary granulator using a new Magnetic Particle Tracking measurement setup. In Chapter 2, theoretical background information is presented. The principle of fluidization of particles is explained as well as the applications of fluidization in industrial processes. Furthermore, the principle of the rotary granulator process is illustrated. The description as well as the advantages and disadvantages of different measurement methods for the investigation of complex gas-solid flows as well as different theoretical approaches for

the description of the particle dynamics in gas-solid flows (including mixing description and convection-dispersion model) are also discussed in this chapter. Finally, the theoretical principles of CFD-DEM simulation are presented.
The experimental setup of the rotary granulator as well as the additional equipment used in the experimental studies are described in Chapter 3. In this chapter, the rotary granulator itself is discussed, a detailed description of the Magnetic Particle Tracking Systems is given in Chapter 4, which also deals with the processing and evaluation of the MPT measurement results, the selection and production of the particles and the validation of the measurement accuracy. For the accuracy validation, in addition to a standard evaluation of the static position detection quality, a newly developed method for the validation of dynamic behavior is presented.
In Chapter 5, the methods and procedures of the Magnetic Particle Tracking investigations are explained. A detailed analysis of the particle properties is described. Subsequently, the experimental investigations and the parameters for the CFD-DEM simulations are presented.
In Chapters 6, the results of the investigations will be presented, analyzed and discussed. The results are to be examined for the influence of liquid on the dispersion behavior in the rotor granulator process. In addition to the experimental results, the investigations from the CFD-DEM simulations will also be used for this purpose. At last, the measurement system will be used to measure transient processes for the first time.
A summary of the important results and the whole thesis will be presented in Chapter 7.

2

Theoretical Background

In the following chapter, the theoretical background of this thesis is presented. First, the principle of fluidization is explained, focusing on the theoretical principles behind the phenomenon. Then the industrial application of fluidization are described, in particular the different designs of fluidized beds. Further topics deal with the complex behavior of particles in dense, gas-solid flows as well as the possibilities for describing this behavior and the measurement methods for tracking particles in these flows.

2.1 Principle of Fluidization

Fluidization is the phenomenon whereby the behavior of solid particle collectives can be changed with the aid of a fluid flow (gas or liquid), whereas the particle collective obtains additional, fluid-like properties (Kwauk, 1992; Fan et al., 1998). Considering a single particle, the fluidization state is reached when the influence of the gravitational force of the particle is overcome by the fluid flow. The drag force as well as the buoyancy of the particle are the forces who counteract the gravity force. An overview of the three relevant forces is given below:

$$\text{Drag force:} \qquad F_\mathrm{d} = \left(\frac{\pi \cdot d_\mathrm{p}^2}{4}\right) C_\mathrm{D} \, \frac{u_\mathrm{f}^2 \cdot \rho_\mathrm{f}}{2}\,, \tag{2.1}$$

$$\text{Buoyancy:} \qquad F_\mathrm{b} = \left(\frac{\pi \cdot d_\mathrm{p}^3}{6}\right) \rho_\mathrm{f}\, g\,, \tag{2.2}$$

$$\text{Graviational force:} \qquad F_\mathrm{g} = \left(\frac{\pi \cdot d_\mathrm{p}^3}{6}\right) \rho_\mathrm{s}\, g\,. \tag{2.3}$$

In addition to the particle diameter d_p, the drag force is particularly dependent on the fluid properties (velocity u_f and density ρ_f) and the so-called drag coefficient C_D. The drag coefficient can be calculated as a function of the flow Reynolds number Re_f, which is dependent on both the flow regime and the particle shape. The buoyancy

force and the gravitational force depend in particular on the volume of the particle. Fluidization occurs when the sum of the drag force (which is usually the significantly larger force) and the buoyancy force is greater than the gravitational force of a single particle. A schematic of the behavior during fluidization of a single particle is shown in Figure 2.1.
Nowadays, especially the flow through particle heaps plays an industrial role. In addition to the force balance on the individual particle level, the collective behavior of particles must be taken into account as well. The fluidization of particle collectives, the so-called fluidized bed, is explained below.

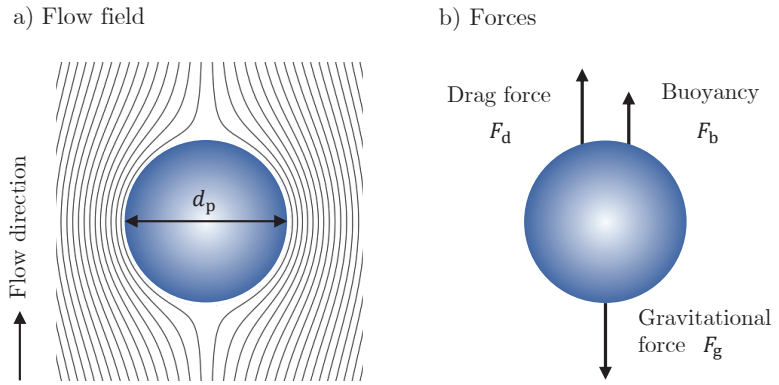

Figure 2.1: Single particle in laminar flow (a) and the forces acting on the particle (b), illustrating the principle of fluidization.

2.1.1 Fluidization of Particle Collectives - Fluidized Beds

A fluidized bed is a type of reactor in which a fluid flows through a heap of particles, the so-called fixed bed. In the following, a gas fluidized bed, or more precisely an air-driven fluidized bed, is assumed, although liquids are also used for fluidization. Depending on the volume flow (and the velocity respectively) of the air flowing through the particle bed, the appearance and behavior of the fluidized bed changes, which is shown in Figure 2.2. Without air supply, a bed of particles forms the fixed bed (a). As the air velocity increases, the fixed bed initially expands without any visible bubble formation (b). At this point the air velocity is high enough, that drag force and buoyancy are greater than the gravitational forces and fluidization occurs. The corresponding air velocity is called the minimum fluidization velocity u_{mf}. If the gas velocity is increased further, bubble formation occurs (c). If the diameter of the fluidized bed is small enough, the bubble diameter can reach the dimensions of the

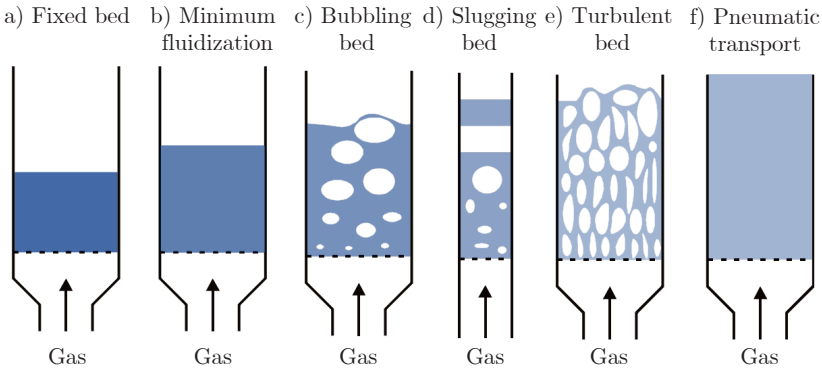

Figure 2.2: Fluidization behaviour as a function of the gas velocity, which increases from left to right (Kunii and Levenspiel, 1991; Dechsiri, 2004).

plant diameter, resulting in slug flow (d). At even higher gas velocities, the entire fluidized bed is interspersed with bubbles, meaning that turbulent flow (e) sets in until the fluidized bed has expanded to such an extent that particles are discharged from the reactor. This can be used for pneumatic transport of the particles (f).

In the following, the theoretical principles for the design and calculation of fluidized beds will be discussed in detail, which includes the calculation of the pressure drop of the fluidized bed, the characterization of the fluidization behavior of different materials as well as the determination of the minimum fluidization velocity.

2.1.2 Pressure Drop

To calculate the pressure drop in a fluidized bed, a distinction must be made as to whether it is a fixed bed or a fully fluidized bed. The course of the pressure drop as a function of the gas velocity for both cases is shown in Figure 2.3. For a fully fluidized bed, the pressure drop is approximately constant. In this range, the pressure loss can be determined using the following equation:

$$\Delta p_{\mathrm{fb}} = g\,(\rho_{\mathrm{s}} - \rho_{\mathrm{f}})\,(1-\varepsilon)\,h_{\mathrm{fb}}\,. \tag{2.4}$$

The pressure loss Δp_{fb} of a fully fluidized bed is thus only dependent on the densities of the solid and the gas (ρ_{s} and ρ_{f}), the height of the particle bed h_{fb} and the porosity ε of the particle bed. The porosity is defined as the ratio of the void volume V_{void}, which corresponds to the volume occupied by the fluid to the total

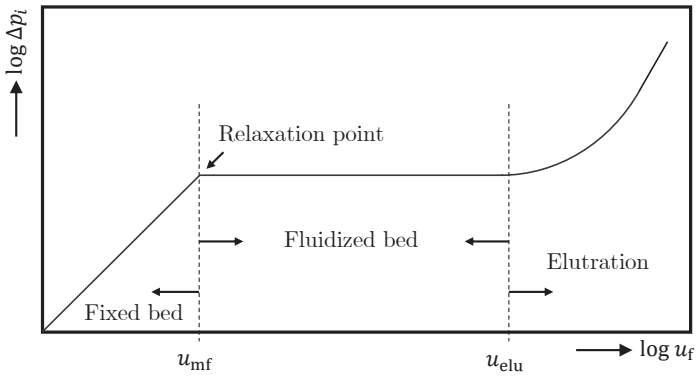

Figure 2.3: Pressure drop of a fluidized bed as a function of gas velocity (Jakubith, 1998).

volume V_{total} of the bulk heap, which is the sum of the volumes of solid and fluid:

$$\varepsilon = \frac{V_{void}}{V_{total}} = \frac{V_f}{V_f + V_s} \,. \tag{2.5}$$

The porosity does not dependent on the particle diameter, but on the type of packing of the particles, which is mainly determined by the shape factor of the particles. It can range from 0.48 to 0.26 in bulk heaps (Kudra and Strumillo, 1998). As the bed expands due to increasing gas volume flow, both the porosity in the particle bed as well as the height of the fluidized bed change to the same extent, which has to be taken into account when calculating the pressure drop of a fluidized bed.

The determination of the pressure loss of a fixed bed Δp_{fix} below the minimum fluidization velocity is considerably more complex. For this purpose, the Ergun equation is used (Wirth, 2019):

$$\Delta p_{fix} = 150 \frac{(1-\varepsilon)^2}{\varepsilon^3} \frac{\eta_f u_f}{d_p^2} h_{fb} + 1.75 \frac{1-\varepsilon}{\varepsilon^3} \frac{\rho_f u_f^2}{d_p} h_{fb} \,. \tag{2.6}$$

In contrast to Equation (2.4), not only the porosity and the densities of the materials play a role in this equation, but also the air velocity u_f and the particle diameter d_p. The Ergun equation covers the laminar flow in the particle bed with the first part of the equation ($\Delta p_{fix} \propto u_f$), while the second term covers the turbulent flow ($\Delta p_{fix} \propto u_f^2$). In order to determine a representative value for the particle diameter for particles that possess a size distribution, the so-called Sauter mean diameter d_{sa} is introduced. This diameter represents the diameter of a sphere that has the same

specific surface area as all of the particles of the bulk heap and is defined as:

$$d_{\mathrm{sa}} = \frac{1}{M_{-1,3}} = \frac{1}{\sum\limits_{i=1}^{n} x_{\mathrm{m,i}}^{-1} \cdot q_{3,i} \cdot \Delta x_i} \,. \tag{2.7}$$

The values for the calculation of the Sauter mean diameter can be taken from a particle size distribution of the material, which is determined experimentally. In the following the particle diameter d_{p} is always to be understood as the Sauter mean diameter, as only bulk materials are examined which possess a distribution of particle sizes in this thesis.

2.1.3 Determination of the Minimum Fluidization Velocity

The minimum fluidization velocity u_{mf}, which is the velocity at the relaxation point (see also Figure 2.3), can be determined using several approaches. First of all, the Ergun equation, given in Equation (2.6), can be used with the assumption that the pressure drop at the relaxation point is equal to the pressure drop of the completely fluidized bed (Equation (2.4), which leads to:

$$\Delta p_{\mathrm{fix}}(u_{\mathrm{mf}}) = \Delta p_{\mathrm{fb}} \,, \tag{2.8}$$

$$\Leftrightarrow \quad 150 \, \frac{(1-\varepsilon_{\mathrm{mf}})^2}{\varepsilon_{\mathrm{mf}}^3} \, \frac{\eta_{\mathrm{f}} \, u_{\mathrm{mf}}}{d_{\mathrm{p}}^2} + 1.75 \, \frac{1-\varepsilon_{\mathrm{mf}}}{\varepsilon_{\mathrm{mf}}^3} \, \frac{\rho_{\mathrm{f}} \, u_{\mathrm{mf}}^2}{d_{\mathrm{p}}} = g \, (\rho_{\mathrm{s}} - \rho_{\mathrm{f}})(1-\varepsilon_{\mathrm{mf}}) \,. \tag{2.9}$$

With this equation, the minimum fluidization velocity u_{mf} can be calculated. The porosity $\varepsilon_{\mathrm{mf}}$ at the relaxation point must be either determined experimentally or be estimated. According to Wirth (2019), however, this determination of the minimum fluidization velocity shall only be used as an approximation, since the porosity at the point of relaxation is difficult to determine precisely. In contrast, correlations are often used to determine the Reynolds number $\mathrm{Re}_{\mathrm{mf}}$, which does not dependent on porosity, but on the Archimedes number Ar and thus on the material properties of the solid and fluid materials. A commonly used correlation was developed by Wen and Yu (1966), who have obtained an estimate of the minimum fluidization porosity from empirical investigations, which simplifies Equation (2.9) as follows:

$$\mathrm{Re}_{\mathrm{mf}} = 33.7 \, \left(\sqrt{1 + 3.6 \cdot 10^{-5} \, \mathrm{Ar}} - 1 \right) \,, \tag{2.10}$$

$$\text{with} \qquad \mathrm{Ar} = \frac{(\rho_{\mathrm{s}} - \rho_{\mathrm{f}}) \, g \, d_{\mathrm{p}}^3}{\rho_{\mathrm{f}} \, \nu_{\mathrm{f}}^2} \qquad \text{and} \qquad \mathrm{Re}_{\mathrm{mf}} = \frac{u_{\mathrm{mf}} \, d_{\mathrm{p}}}{\nu_{\mathrm{f}}} \,. \tag{2.11}$$

In addition to this correlation, other equations for determining the Reynolds number exist, for example the correlations by Gorosko et al. (1958). Furthermore, it is possible

to determine the minimum fluidization velocity graphically with the so-called Reh diagram, which has proven to be a good approximation method (Reh, 1961). However, it is recommended to determine the velocity experimentally (Wirth, 2019).

In process applications, the gas volume flow is often specified instead of the gas velocity, since the volume flow rate is geometry-independent and depends only on the ventilator settings and performance. In order to ensure quick comparability, the dimensionless, normalized gas velocity u^* is specified additionally, which is defined according to Wen and Yu (1966) as

$$u^* = \frac{u_\mathrm{f}}{u_\mathrm{mf}}\,. \tag{2.12}$$

This parameter relates the actual fluid velocity to the velocity u_mf required for fluidization, allowing the intensity of fluidization to be estimated on the basis of this parameter.

2.1.4 Fluidization Behavior of Different Materials

The most commonly used method for the characterization the fluidization behavior of various powders is the Geldart classification (Geldart, 1973). Here, the density difference (ρ_s - ρ_f) between solid and fluid as well as the average particle diameter are required. Through extensive experimental investigations, Geldart has distinguished four groups, the Geldart particles A, B, C and D, which each are characterized by a distinctive fluidization behavior. The diagrams in Figure 2.4 are usually utilized to classify materials into the various groups on the basis of their material properties (Vasconcelos and Amarante Mesquit, 2011). The distinctive fluidization behavior for each Geldart group is described in the following (Geldart, 1973).

Particles of the Geldart group A (*aeratable*) possess a low density (mostly below $1.4\,\mathrm{g\,cm^{-3}}$ and/or a mean particle diameter smaller than 100 µm. The fluidization behavior is characterized by the fact that the fixed bed initially expands uniformly with increasing gas velocity. At a gas velocity greater than the minimum fluidization velocity, bubble formation sets in, leading to a high mixing of the fluidized bed. If the gas supply is interrupted abruptly, the particle bed collapses slowly.

Particles with a higher density ($1.4 < \rho_\mathrm{s} < 4\,\mathrm{g\,cm^{-3}}$) and a mean particle diameter of 40 to 500 µm are particles of the Geldart group B, which are also referred to as *sand-like*, since typical representatives of this group are sands. The velocity of the gas, which is necessary for the formation of bubbles, is slightly higher than the minimum fluidization velocity, and the growth of the bubbles is not limited. If the gas supply is stopped, the bed collapses quickly.